Published in final edited form as:
Dev Biol. 2011 May 1; 353(1): 120–133. doi:10.1016/j.ydbio.2011.01.031.

Lineage analysis of micromere 4d, a super-phylotypic cell for Lophotrochozoa, in the leech *Helobdella* and the sludgeworm *Tubifex*

Stephanie E. Gline[a,*], **Ayaki Nakamoto**[b], **Sung-Jin Cho**[a], **Candace Chi**[a], and **David A. Weisblat**[a]

[a] Dept. of Molecular and Cell Biology, 385 LSA, University of California, Berkeley, CA 94720-3200, USA

[b] Dept. of Molecular and Cellular Biology, Univ. of Arizona, Tucson, AZ, 85721, USA

Abstract

The super-phylum Lophotrochozoa contains the plurality of extant animal phyla and exhibits a corresponding diversity of adult body plans. Moreover, in contrast to Ecdysozoa and Deuterostomia, most lophotrochozoans exhibit a conserved pattern of stereotyped early divisions called spiral cleavage. In particular, bilateral mesoderm in most lophotrochozoan species arises from the progeny of micromere 4d, which is assumed to be homologous with a similar cell in the embryo of the ancestral lophotrochozoan, more than 650 million years ago. Thus, distinguishing the conserved and diversified features of cell fates in the 4d lineage among modern spiralians is required to understand how lophotrochozoan diversity has evolved by changes in developmental processes. Here we analyze cell fates for the early progeny of the bilateral daughters (M teloblasts) of micromere 4d in the leech *Helobdella* sp. Austin, a clitellate annelid. We show that the first six progeny of the M teloblasts (em1–em6) contribute five different sets of progeny to non-segmental mesoderm, mainly in the head and in the lining of the digestive tract. The latter feature, associated with cells em1 and em2 in *Helobdella*, is seen with the M teloblast lineage in a second clitellate species, the sludgeworm *Tubifex tubifex* and, on the basis of previously published work, in the initial progeny of the M teloblast homologs in molluscan species, suggesting that it may be an ancestral feature of lophotrochozoan development.

Keywords

Micromere 4d; Mesoderm; Endoderm; Leech; Annelid; Spiralian; Lineage tracing

Introduction

A central question in developmental biology is that of how changes in developmental processes underlie the diversification of body plans evident in extant animals. For addressing this question, spiralian taxa (Mollusca, Annelida, Platyhelminthes, Nemertea, and Entoprocta and others) provide species with homologous cells in their early embryos that lead to a remarkably diverse set of adult body plans. They share a characteristic pattern of early embryonic cell divisions (spiral cleavage) that is now regarded as an ancestral character of the super-phylum Lophotrochozoa (Dunn et al., 2008; Hejnol et al., 2009). In

*Corresponding author at: Present address: Dept. of Orthopaedic Surgery, University of California, San Francisco, CA, U-470, San Francisco, CA 94143-0514, USA., stephgline@gmail.com (S.E. Gline).

spiral cleavage, the second embryonic axis is established by specifying one quadrant of the embryo as the unique “D quadrant” (by cell interactions in equal cleavers or by the segregation of determinants in unequal cleavers (Freeman and Lundelius, 1992). Micromere 4d, arising within the D quadrant at the sixth cleavage, typically divides equally to form left and right precursors of bilaterally symmetric mesoderm (but see Meyer et al., 2010), and thus provides an example of inter-phyletic homology at the single cell level that has no known parallel in the other metazoan super-phyla.

In the leech *Helobdella*, a clitellate annelid, micromere 4d is designated proteloblast DM″ ; its bilateral division gives rise to two large stem cells (M teloblasts), whose iterated divisions yield precursors (m blast cells) of the segmental mesoderm (Fernández and Stent, 1980; Zackson, 1982; Weisblat and Shankland, 1985; Bissen and Weisblat, 1989). Beyond this segmental contribution, early progeny of the M teloblasts also contribute to the unsegmented prostomium at the anterior (Anderson, 1973; Zackson, 1982; Gleizer and Stent, 1993). This contribution is of particular interest for comparative studies because it arises relatively early on in the 4d lineage and thus might be expected to show greater conservation across species. The prostomial contribution of the M lineage was poorly defined in these early studies, however, due in part to technical limitations.

Knowledge of the early mesodermal lineages is also necessary for understanding segmentation in leeches and allied taxa. In vertebrates and insects, segments are formed by creating boundaries within fields of initially equipotent cells. In clitellate annelids by contrast, segments represent the extensive interdigitation of spatially stereotyped clones arising from cells in five longitudinal arrays of m, n, o, p and q blast cells; the blast cells arise from a teloblastic posterior growth zone (see Weisblat and Shankland, 1985; Wedeen and Shankland, 1997 for further details). Leech segments may be defined either in terms of the septa arising from the mesodermal hemisomites or in terms of the ganglionic repeats within the ventral nerve cord, which straddle the septa; hence the boundaries of neural and mesodermal segments are out of phase with one another; the first purely segmental mesodermal hemisomite is the one that straddles the first two segmental ganglia (R1 and R2). Here, we employ the neural definition of segment boundaries in keeping with most current workers and because the ganglia are more reliably observed throughout development.

The interdigitation of serially homologous clones means that segments at the anterior end of the animal do not receive the complement of cells that would normally be contributed by yet more anterior blast cell clones. This interdigitation is most pronounced for the m blast cell clones, whose definitive progeny span 3 segments in the mid-body of the animal (Weisblat and Shankland, 1985). Does the embryo compensate for the lack of the normal mesodermal complement in the anteriormost segments, and if so, how?

Here, using high-resolution cell lineage tracing techniques, we have studied the early progeny of the M teloblasts in greater detail. We show that, prior to initiating the production of purely segmental m blast cells (sm cells), each M teloblast produces six early mesodermal cells (em cells), which contribute wholly or in part to non-segmental mesoderm. As previously described, all sm cells undergo identical stereotyped early divisions and give rise to homologous sets of pattern elements whose position along the anterior/posterior axis is determined by the birth order of their blast cell of origin (Fig. 1; Weisblat and Shankland, 1985; Gleizer and Stent, 1993). In contrast, the six em cells fall into five groups that differ from each other and from standard sm cells in their early division patterns (with the exception of em6 whose early divisions are indistinguishable from sm cells); each em cell type contributes a distinct component to the later embryo. In addition, we show that em5 and

em6 give rise to hybrid clones, contributing cell types to the first two segments that in midbody segments would be provided by the interdigitation of more anterior m clones.

A parallel re-examination of the 4d lineage in the oligochaete *Tubifex* reveals that in this annelid, too, cell 4d contributes to anterior non-segmental tissue. These two worms have different foregut morphologies and thus distinct anterior contributions from 4d. These differences further illustrate the principle that changes in the developmental program of the 4d lineage are associated with the diversity of spiralian body plans.

Materials and methods

Embryos

Embryos of *Helobdella* sp. (Austin; Hau) collected from Austin, Texas, were obtained from a laboratory breeding colony. Embryos were cultured in HL saline and maintained at 23 °C as previously described (Song et al., 2002). Staging and cell nomenclature are as defined previously for *H. robusta* (Weisblat and Huang, 2001) however there are species specific differences in the cell cycle rates between *H. robusta* and the species used in this study *H.* sp. (Zhang and Weisblat, 2005; Gonsalves and Weisblat, 2007). Embryos of *Tubifex tubifex* were collected as previously described in (Shimizu, 1982).

Plasmid injection, mRNA synthesis, and mRNA injection

pEF-H2B:GFP plasmid (Gline et al., 2009) was injected at a concentration of 96 ng/ul with 3 mg/ml fixable tetramethylrhodamine dextran (RDA; Molecular Probes, Eugene, OR). h2bGFP mRNA was transcribed in vitro as previously described (Gline et al., 2009). The concentration of mRNAs in the needle was 0.5 mg/ml with 3 mg/ml RDA. Fixable Alexa fluor 647 dextran (ADA) was injected at a concentration of 1 mg/ml and fixable fluorescein-conjugated dextran (FDA) at 5 mg/ml.

Microscopy

For time-lapse fluorescence and darkfield microscopy, injected embryos were mounted in HL saline, then examined and photographed using a Nikon E800 epifluorescence microscope equipped with a CCD camera (Princeton Instruments, Trenton, NJ), controlled by MetaMorph software (Molecular Devices, Sunnyvale, CA). Fluorescent and/or darkfield images were acquired every 2–5 min. For confocal microscopy, embryos were fixed for 1 h at RT or o/n at 4 °C in 0.75×PBS in 4% paraformaldehyde. Images were acquired on a Leica SMRE microscope equipped with a TCS SL scanning head. Stacks of confocal images were processed using Image J (Jackson et al., 2001) for color merging and Z-projections.

In situ hybridization and immunostaining

GFP immunostaining was performed as in (Gline et al., 2009). Immunostaining against histone H1 was done as for GFP with the following changes; mouse monoclonal antibody against histone H1 (Chemicon, MAB052) was used at 1:1000 and alexa fluor 488 conjugated goat anti-mouse secondary was used at 1:500.

Helobdella tropomyosin (*tropo1* and *tropo2*), and *hedgehog* (*hh*) genes were identified from the *H. robusta* whole genome assembly (http://genome.jgi-psf.org/Helro1/Helro1.home.html). PCR primers were designed based on the sequence information obtained from the genome assembly (*tropo1* forward: ATTAAGAAGAAGGTGCACACGATGAAGACT; *tropo1* reverse: CAGCTCGGTGAATGTGAAATCGAGTTCGTT; *tropo2* forward: ACAGGAGGAAGTGCCTTATCAACATTAAAA; *tropo2* reverse: GGCAATTTCATTGAACGCATTCTCCAATTC; *hh* forward:

ATGGAGAGTGTAGCAGATGAC; *hh* reverse: GGAGCAATGAATAT-GACTCCT). Partial cDNA fragments of *tropo1*, *tropo2*, *and hh* were amplified from *H.* sp. Austin cDNA, gel extracted and cloned into pGEM-T Easy (Promega). These sequences were designated as *Hau-tropo1* (HQ161082), *Hau-tropo1* (HQ161083), and *Hau-hh* (AAM70491). Riboprobes labeled with digoxygenin were made using the MEGAscript (Ambion) kit, according to the manufacturer's instructions.

For fluorescent in situ hybridization (FISH) stage 10 embryos were collected and relaxed for 10 min in a relaxant solution (10 mM $MgCl_2$, 5 mM NaCl, 1 mM KCl in 8% ethanol in water), then fixed in 4% paraformaldehyde (PFA) for 1 h. Embryos were processed for in situ hybridization as described (Cho et al., 2010) with the following changes. Probe concentrations ranged from 1.0 to 2.0 ng/μl and hybridization was carried out overnight at 67 °C in a 1:1 mixture of deionized formamide and 5× SSC, 0.2 mg/ml tRNA, 0.1 mg/ml heparin, 1× Denhardt's solution, 0.1% Tween 20 and 0.1% CHAPS. Probe lengths were as follows: *Hau-tropo1* (813 bp), *Hau-tropo2* (735 bp), and *Hhr-hh* (1113 bp).

Subsequently, the NEN Tyramide Signal Amplification (TSA™) Plus kit (Perkin Elmer, Wellesley, MA, USA) was used as described (Cho et al., 2010). FISH-processed embryos were co-stained with DAPI (4′,6-Diamidino-2-phenylindole, sigma) to visualize cell nuclei.

Embedding and sectioning

Selected embryos were dehydrated (through a graded ethanol series into propylene oxide), then infiltrated with epoxide embedding medium according to the manufacturer's instructions (Poly/Bed 812; Polysciences). Thick sections were cut by hand using a razor blade.

Results

Six early m (em) blast cells contribute non-segmental progeny

Helobdella embryos exemplify a version of unequal spiral cleavage that is highly conserved among leeches and oligochaetes (clitellate annelids; (Sandig and Dohle, 1988; Dohle, 1999; Bissen and Weisblat, 1989; Shimizu, 1982; Storey, 1989) and to a lesser extent with more distantly related annelids (Dohle, 1999). Three rounds of division in the A, B and C quadrants produce typically small micromeres. The D quadrant, which is specified by the inheritance of RNA rich, yolk deficient cytoplasm during the first two unequal cleavages (Fernández et al., 1990; Astrow et al., 1987; Ren and Weisblat, 2006; Lyons and Weisblat, 2009), undergoes four rounds of spiral cleavage. But the second and fourth micromeres (micromeres 2d and 4d in classical terminology) are disproportionately large in clitellate embryos (Figs. 1; 2A). In *Helobdella*, micromeres 2d and 4d are designated DNOPQ and DM ″, respectively (Fig. 1A). DNOPQ produces four bilaeral pairs of ectodermal segmentation stem cells (left–right pairs of N, O/P, O/P and Q teloblasts), plus other small cells (Figs. 1A, B). DM divides bilaterally, similar to the 4d cells in many other spiralians (Figs. 1; 2A, B); its progeny are mesodermal segmentation stem cells (M_L and M_R teloblasts), which are the focus of this work.

Each teloblast undergoes iterated, highly unequal stem cell divisions, producing a coherent, age-ranked column (bandlet) of blast cells (Fig. 1B; Figs. 2C–E). For the most part, blast cells undergo lineage-specific stereotyped patterns of asymmetric cell divisions and contribute serially homologous pattern elements to segmental tissues, with the clones of early arising blast cells contributing to anterior segments and later born clones to more posterior segments (Figs. 1B, C).

Previous work indicated that some early progeny of the M teloblasts make anterior non-segmental contributions (Zackson, 1982; Gleizer and Stent, 1993; Gline et al., 2009); consistent with this, we observed morphological features of anterior mesoderm not seen in segments (Figs. 2F–H). To further define and characterize the early progeny of the M teloblasts, we used the purely segmental ectodermal OP lineage (Kuo and Shankland, 2004) as a landmark to define the anterior limits of segmentation and thereby assayed the extent to which the M lineage extends anterior to the segmental ectoderm. Thus, we injected ipsilateral M teloblast and OP teloblast with different fluorescent lineage tracers immediately after their births (15.5 h and 34 h AZD, respectively), and then fixed the resultant embryos at various times to examine the distribution of fluorescently labeled cells. For consistency, the M_L teloblast was targeted in all unilateral injections reported here.

Thirty hours after injection of the M teloblast, the M- and OP-derived bandlets were not yet in contact (Fig. 3A). By 48 h post-injection, the distal portion of the OP lineage overlay the M lineage, but their anterior boundaries did not align; the anterior edge of the OP lineage lay posterior to the anterior M lineage (Fig. 3B). By 72 h post-injection, the anterior M lineage was morphologically distinct from the more posterior portion that lay beneath the segmental OP lineage (Fig. 3C). By 164 h post-injection (stage 10), the anteropos-terior progression of segment differentiation is evident and the mismatch between the anterior limits of the M and OP lineages remains (Fig. 3D), indicating that the M lineage anterior to the OP boundary is non-segmental. Embryos in which DM″ was co-injected with RDA and a plasmid encoding a histone:GFP fusion protein (pEF-H2B:GFP) to mark the nuclei of individual cells in the labeled lineage revealed that hundreds of DM″ derived cells were present in the developing head by stage 9 (5 days post-injection; Fig. S1).

Because the M teloblasts are born ~6.5 h before the N teloblasts and ~12.5 h before the OP proteloblasts and Q teloblasts, it was previously assumed that segmental blast cell production began earlier in the mesodermal lineage than in the ectodermal lineages. Given the finding that the early mesodermal (em) lineage contributes so substantially to anterior non-segmental tissues, we used further pairwise injections of M, N and OP teloblasts to re-examine the relative timing at which the production of segmental founder cells begins in all teloblast lineages. These experiments revealed that production of segmental founder cells in both mesoderm and ectoderm begins within a narrow time window corresponding to stage 6b (Figs. 3E, F; Fig. S2).

Time lapse videos were used to determine the number of “early mesoderm” (em) cells born prior to stage 6b and to correlate the birth of each em cell with the easily observed cleavages of ectodermal proteloblasts, to facilitate further experiments. In these videos, the rhythmic shape changes associated with cytokinesis of the teloblasts showed that the M teloblasts undergo 6 cytokineses prior to the beginning of stage 6b, when the first definitive sm cell is born (Fig. 1D; Movie S1). No significant difference was found in M teloblast cell cycle durations during em production or between em and sm production; average cell cycle durations were calculated for the first ten divisions of the M teloblast after the birth of em1, with an overall average cell cycle of 120 min (Fig. 1D). The minimum average was 116.6 (±22.9) min (for em5) and maximum 127.6 (±20.8) min (for em4). The duration of the M teloblast cell cycle leading to the birth of em1 could not be determined directly from time-lapse recording due to technical reasons.

Characterization of the em cell lineages

To test the conclusion that the M teloblasts generate six early mesoderm (em) cells prior to the first segmental mesoderm (sm) blast cells, and to visualize the clonal descendants of these putative em cells, progeny of individual em or sm cells were uniquely labeled using timed tandem injections. For this purpose, M teloblasts of carefully staged embryos were

first injected with RDA and either pEF-H2B:GFP plasmid or *h2b:gfp* mRNA, to mark cytoplasm and nuclei, respectively. Two hours later, after one RDA-labeled blast cell was produced, the teloblast was re-injected, with AlexaFluor 647 dextran (ADA) tracer, so that the cytoplasm of all ensuing blast cells would be double-labeled. Data from the time-lapse experiments described earlier were used to determine the timing of the tandem injections. Shifting these tandem injections later into development permitted us to label individual em (and sm) cells uniquely, and fixing the resultant embryos at different stages allowed us to view the uniquely labeled clones at a variety of clonal ages (Fig. 4). These experiments confirmed that six em cells (henceforth designated em1 through em6) are born prior to the first sm cell, and also revealed that these six em cells contribute five distinct sets of cells to the late embryo. The fates of these cells are summarized later, preceded by a description of a typical sm clone for comparative purposes:

sm

Contributions of segmental m blast cells (sm cells) to the later stage embryo have been characterized previously (Kramer and Weisblat, 1985; Weisblat and Shankland, 1985; Bissen and Weisblat, 1989; Gleizer and Stent, 1993). The first division of an sm blast cell occurs at clonal age 13–15 h in *H.* sp. (Austin) and is roughly equal, yielding sister cells lying side by side within the m bandlet (Fig. 1B; Fig. S3; our unpublished observations). By 48 and 72 h clonal age, these clones averaged 10.1+/−2.96 and 41.5+/−6.7 cells, respectively (Figs. 4G–G″; 5). At stage 9, the typical midbody sm cell clone includes muscle and mesenchymal cells lining the coelom and associated with the ventral nerve cord, nephridia, and a small cluster of neurons in each ganglion Figs. 1C, D; 6 Q–S; (Weisblat and Huang, 2001); each clone is distributed across parts of three adjacent segments, so that the M teloblast-derived progeny in any given midbody segment include subsets of three interdigitated sm clones Figs. 1C; 6 Q–S; (Weisblat and Huang, 2001). In addition to these segmental progeny, each sm clone generates circumferential muscle fibers to the provisional integument; these cells often lie several segments posterior to iso-clonal cells within the germinal plate (Fig. 6Q). As will be seen later, the fates of cells em1–em4 differ dramatically from the sm cells, while em5 and em6 make a mix of segmental and non-segmental contributions.

em1 and em2

The progeny of em1 and em2 behave similarly throughout development; both undergo early rounds of seemingly equal cell divisions to generate scattered clones of morphologically indistinguishable “freckle cells” beneath a micromere-derived epithelium between the germinal bands in the early stage 8 embryo as previously described for *H. triserialis* and *H. robusta* (Figs. 4A–A″, B–B″; Zackson, 1982; Chi, 1996). Most em1 clones comprised fewer cells than most em2 clones at both two and three days clonal age (1.7+/−0.5 vs. 4.3+/−1.1 cells at 2 days and 8.7+/−2.3 vs. 13.8+/−2.1 cells at 3 days, for em1 and em2 clones, respectively; Fig. 5). Microinjection may cause minor developmental delays in the injected lineages and the new born M teloblasts are particularly sensitive to this effect, which would selectively depress the cell counts for em1 clones; thus, the apparent differences in proliferation between em1 and em2 may be an experimental artifact, and the maximum observed clone size may reflect normal development more accurately than the average clone size in these experiments. Accordingly, there were several embryos with comparable cell counts for em1 and em2 clones at 3 days clonal age (14 and 16 cells maximum, respectively; Fig. 5).

At early stage 9, progeny of em1 and em2 constitute a cluster of cells where the lumen of the proboscis is forming and a disperse set of flattened mesenchymal cells lining the yolk (Figs. 6A–C, and data not shown). By late stage 9, almost all the progeny of em1 and em2

comprise a continuous population of cells lining the lumen of the proboscis and extending between the germinal plate and the yolk syncytium (Figs. 7A, B). By stage 11 when gut morphogenesis has taken place, these cells have come to line the crop, intestine and rectum, as well as the lumen of the proboscis (Figs. 8A–C). Some cells from any labeled em1 or em2 clone were seen contralateral to the injected side within the proboscis, and at the level of the midgut and hindgut, the em1 and em2 clones were distributed uniformly across the midline, reflecting an intermingling of em1 and em2 clones from the left and right sides of the embryo (Figs. 8B, C). In summary, the progeny of em1 and em2 line the gut throughout its anteroposterior extent.

em3

Proliferation of the em3 clone is slower than any other em lineage. This clone comprises exactly 2 cells at 48 h and only 4.3+/−0.5 cells by 72 h clonal age (Figs. 4C–C″; 5). In contrast to the em1 and em2 clones, the first em3 divisions are markedly unequal; one cell is invariably larger and sits at the dorsal anterior edge of the M lineage (Figs. 4C–C″).

In stage 9 embryos, em3 contributes to cells in the developing proboscis (Figs. 6D, E), which by late stage 9 are recognizable as presumptive radial muscle cells within dorsal part the proboscis (Figs. 7C, D). Cell em3 also contributes a patch of cells at the lateral edge of the developing head (Figs. 6D–E). In all embryos the tracer in this patch was brighter than the rest of the clone, suggesting that there had been fewer cell divisions and/or less cell growth in this sub-lineage (so that the tracer had remained more concentrated). At later stages, the brightly labeled patch appeared as a dense ball, the position of which varied widely in the A–P axis (Fig. 7E and data not shown), suggesting that it had detached and was floating within the coelom.

em4

At 48 h clonal age, the em4 clone comprises 4.6+/−1.4 adjacent cells of roughly equal size along the A–P axis of the M lineage (Figs. 4D–D″; 5). By 72 h clonal age this clone averages 15.7+/−1.2 cells (Fig. 5), still of roughly equal size, and has taken on a distinctive bipartite morphology. At the anterior dorsal portion of the clone is an arc of 3–4 cells; the rest of the clone forms a compact cluster at the base of the arc (Fig. 4D′–D ″). In stage 9 embryos, em4 contributes scattered cells throughout the head including mainly lateral radial muscles within the proboscis (Figs. 6F–H; 7F, G), and also a sparse population of cells with extended processes, lying among the circumferential muscle fibers of the provisional integument (Fig. 6I). Based on their morphology, which differs from that of the sm-derived circumferential muscle fibers, we speculate that these cells may be neurons innervating provisional circumferential muscle fibers, which initiate peristaltic contractions at this stage.

em5

The progeny of em5 at 48 h clonal age, with an average clonal size of 7.4+/−1.4 cells, exhibit a range of nuclear sizes and comprise a coherent cluster behind the em4 clone at the anterior of the m bandlet (Figs. 4E–E″; 5). By 72 h clonal age em5 comprises on average 22.7+/− 3.5 cells (Fig. 5), some of which are situated beneath the rest of the M lineage and are therefore not visible in maximal projection confocal stacks (Figs. 4E′–E″). In many embryos at 72 h clonal age, there was RDA-containing cell debris anterior to the labeled lineage (Figs. 4E′–E″), suggesting that cell death had occurred in this clone.

In the early stage 9 embryo, most definitive progeny of em5 lie in the non-segmental prostomium, including presumptive radial muscle cells within the proboscis and cells at its tip which are the presumptive musculature of the proboscis sheath (Figs. 6J–L). Similar to em4, em5 also gives rise to a sparse population of cells amongst the provisional

circumferential muscle fibers (Fig. 6M). In the late stage 9 embryo, em5 contributes the majority of muscle fibers in the proboscis sheath (Fig. 7H) and radial muscle fibers in the ventral portion of the outer ring of the proboscis (Fig. 7I).

In contrast to clones derived from cells em1 through em4, which contribute exclusively non-segmental progeny, em5 also gives rise to a small cluster of presumptive neurons on the ipsilateral side of segmental ganglion R1, ventral to the first forming coelomic cavity (hemisomite; Fig. 6L). These cells are similar in position and number to the clusters of M teloblast-derived neurons (mn) in each segmental ganglion (Figs. 1; 6S; Kramer and Weisblat, 1985; Weisblat and Shankland, 1985). Interpreting this cluster of em5-derived cells in the ganglia of R1 as serially homologous to the sm-derived neurons of more posterior ganglia, cell em5 generates a hybrid clone, making minor segmental and major non-segmental contributions.

em6

The em6 clone exhibits many but not all features of the standard sm clones. The cell cycle duration of em6 and the orientation of its mitosis are indistinguishable from those of the sm cells, while the cell cycles for em1–5 are significantly different (Fig. S3). At 48 and 72 h clonal age, the em6 clones comprise an average of 10.3+/−2.6 and 37+/−2.9 cells, respectively, not significantly different from sm clones at equivalent ages (t test; P=0.862 and 0.282 respectively; Fig. 5). At these time points, the em6 clone is also morphologically similar to the true hemisomite arising from the next M-derived cell, sm1 (Figs. 4F–F″, G–G ″).

Analysis of the uniquely labeled progeny of em6 in the stage 9 embryo revealed that em6 gives rise to a nearly complete segment’s worth of progeny spanning segments R1–R3 (Figs. 6N–P). Deeper projections show uniquely labeled em6 progeny surrounding the walls of the nascent coelomic cavity underlying the anterior portion of gangion R1, as well as contributing prospective muscles, a small cluster of M-derived neurons in segment R2, and a lateral patch of mesoderm in segment R3 (Figs. 6N–P).

However, in addition to a largely normal complement of segmental progeny, the em6 clone gives rise to longitudinal muscles within the proboscis, which are especially conspicuous by late stage 9 (Fig. 7H, I). Another difference with respect to the standard sm cells is that em6 does not give rise to any provisional circumferential muscle fibers (compare Figs. 6N and Q). Thus, both the em5 and em6 clones are hybrid in nature, generating mixtures of segmental and non-segmental progeny. Their progeny contribute to the M kinship groups in segments R1 and R2.

em contributions to proboscis

The experiments described earlier revealed that em cells contribute extensively to the proboscis, a muscular, eversible feeding apparatus (Sawyer, 1986). The development of this complex structure provides an interesting example of organogenesis, in which both Hedgehog and Wnt signaling pathways are implicated (Kang et al., 2003; Cho et al., 2010).

At stages 9 and 10, which were used as the end point for much of our work, the proboscis proper is organized into three concentric rings of cells: the inner ring begins as a layer of columnar epithelial cells surrounding the lumen; immediately outside the inner ring is a thin middle ring comprised of presumptive circumferential muscle fibers; the outer ring includes multiple layers of cells including presumptive radial and longitudinal muscle cells, nerves and secretory ductules (Figs. 9, 10).

Previous work has shown that various non-teloblast lineages contribute to the proboscis, accounting for the presumptive circumferential muscle fibers of the middle ring, epithelial cells in the outer ring and in the sheath, and longitudinal cells in the proboscis that were proposed to be muscles and/or neurons (Fig. 10B; Huang et al., 2002; Kang et al., 2003). This prior work left much of the proboscis unaccounted for, including much of the outer ring and all of the inner ring. Moreover, the correspondence between these early cells and the differentiated cell types of the adult proboscis was not certain. Our present work shows that the em lineages contribute most or all of the previously unaccounted for cells and suggest corrections for previous cell fate assignments.

To examine the contributions from the M lineage to the proboscis and its sheath in detail, we injected either DM″ or a newborn M teloblast with RDA. Embryos were cultured to stage 9 or 10, counter-stained with DAPI and observed in thick sections using confocal microscopy.

In DM″-injected embryos, the inner ring appeared as a continuous band of RDA-containing cells, indicating that it derived entirely from DM″ (Figs. 9A–I). Directly surrounding the inner ring were a small number of RDA-labeled circumferential muscle fibers (Figs. 9G–I). The majority of the contributions from DM″ to the outer ring appear to be radial muscle precursors (Figs. 9D–F, J–O). DM″-derived longitudinal muscle fibers were apparent as a ring of puncta just outside the inner ring (Figs. 9G–I). In addition to the proboscis proper, RDA-containing fibers were seen throughout the sheath, including an array of M-derived presumptive longitudinal muscle fibers radiating from the tip of the proboscis into the sheath (Figs. 9A–C). These sheath muscles extend posteriorly (Figs. 9D–F) to the oral opening, where a set of M-derived circumoral muscle fibers run perpendicular to them (data not shown).

By late stage 10, the proboscis has retracted and its lumen is tri-radiate. Embryos with unilateral M injections contained labeled cells on both sides of the midline in all three rings and in the sheath (Figs. 9J–L), indicating that em-derived cells had routinely crossed the midline, a phenomenon that is seldom seen in segmental ectoderm or mesoderm. The extent of midline crossing varied within the different layers of the proboscis and from embryo to embryo.

During stage 10 cellular organization within the proboscis increased. Nuclei of the radial muscle fibers formed a prominent ring near the periphery (Figs. 9J–O). By late stage 10, the nuclei of the radial muscles were surrounded by a ring of smaller nuclei corresponding to the longitudinal muscle fibers, as in the adult (Figs. 9M–O). At earlier time points, presumptive longitudinal muscle fiber nuclei were seen at intermediate radial locations, which we interpret as an outward migration from their initial position next to the middle ring. Contributions of the DM sub-lineages to the proboscis are summarized in Fig. 10.

Previous work (Kang et al., 2003) identified an inner ring of cells in the developing proboscis as the main site of expression for a *Helobdella hedgehog* gene homolog (*Hau-hh*). These cells would thus be a candidate signaling center for organizing the development of the concentric rings of cells comprising the proboscis. Our present results suggest that the cells expressing *Hau-hh* at the core of the proboscis are those arising from the em1 and em2 clones. This was confirmed by examining the sections through the proboscis of embryos whose early M teloblast was injected with FDA and which were then processed for *Hau-hh* in situ hybridization at stage 9 (Figs. 11A–D). *Hau-hh* was also expressed in epidermal cells at the tip of the proboscis where it joins the sheath and in a ring of fibers surrounding the proboscis that resembles the putative longitudinal muscle fibers. It had been suggested (Kang et al., 2003) that the inner ring cells differentiate into the radial muscles; but our present results make this unlikely: first, lineage tracer revealed that the inner ring cells did

not extend processes to the outer surface of the proboscis (Figs. 9J–O), but instead lost their columnar shapes and became progressively more flattened in later stages of development, as if differentiating into an epithelial lining of the proboscis (Figs. 9M–O). Moreover, lineage tracing also revealed that cells arising from em3, em4 and em5 near the outer surface of the proboscis did extend centrally (Figs. 9J–O), consistent with being radial muscle precursors.

Further evidence regarding the nature of the em1 and em2 derivatives came from using the expression of tropomyosin family genes as cell differentiation markers. Tropomyosins are actin binding proteins, paralogs of which are expressed differentially in muscle and non-muscle cells (Pittenger et al., 1994; Perry, 2001). The *Helobdella* genome contains multiple tropomyosin homologs. In situ hybridization revealed that the paralog designated *Hau-trop1* was expressed in segmental muscle cells as they differentiated in anteroposterior progression within the M lineage (Fig. 11E), by M-derived circumferential muscle cells of the provisional integument (Fig. 11E), by the M-derived muscle cells associated with the proboscis sheath and by cells in the outer ring of the proboscis (Figs. 11F–H), suggesting that this gene is a candidate marker for differentiating muscle cells. *Hau-trop1* was also expressed at low levels by the radially oriented cells arising from cells em3, em4 and em5 near the outer surface of the proboscis, consistent with the hypothesis that they are indeed differentiating into the radial muscles, but not by the inner ring cells arising from em1 and em2. Instead, these cells expressed a different tropomyosin paralog, *Hau-trop2*, which was not detected in any of the known muscles listed earlier (Figs. 11I–K). These observations support the conclusion that the radial muscles of the proboscis arise not from the em1 and em2-derived cells of the inner ring, but rather from the em3, em4 and em5 cells in the outer ring at stages 9–10 (Fig. 10).

4d lineage in the oligochaete annelid Tubifex

The sludgeworm *Tubifex* and the leech *Helobdella* differ dramatically in morphology, including head structure. Nonetheless, as clitellate annelids, their embryos undergo homologous early cleavages and the homology between the fate maps of their teloblasts in later development is also unmistakable (Shimizu, 1982; Goto et al., 1999a,b; Nakamoto et al., 2000). Thus, they are useful systems for comparison aimed at relating changes in 4d lineages to the evolution of morphological differences.

Segmental boundaries in *Tubifex* are marked by bundles of chitinous bristles (chaetae). *T. tubifex* has four bundles of chaetae per segment, one dorsolateral pair and one ventrolateral pair (Fig. S4; (Bouche et al., 1997). The first segmental chaetae appear immediately posterior to the peristome (Bouche et al., 1997). There is no ganglion associated with this “segment”, however; the anterior end of the first segmental ganglion is in the next posterior segment (A.N., data not shown). Thus, adapting a neurogenic definition of segmentation as in *Helobdella*, we define the first true segment as the second chaetae-bearing segment, defined elsewhere as segment III (Bouche et al., 1997).

To visualize the mesodermal lineage in *Tubifex*, cell 4d was injected with RDA and embryos were cultured for various intervals prior to fixation. In *Tubifex*, injected cytoplasmic tracers such as RDA are differentially concentrated at the sub-cellular level, thus providing fortuitous nuclear markers (Goto et al., 1999b). As in *Helobdella*, the M teloblasts in *Tubifex* undergo highly asymmetric divisions to give rise to smaller blast cells, born towards the animal pole (Fig. 12A; Goto et al., 1999a). Unlike *Helobdella*, the left and right M bandlets in *Tubifex* do not contact one another at their anterior, distal tips (Fig. 12A, B; Goto et al., 1999b).

After 72 h of development, the anterior portion of the bilaterally symmetric 4d lineage is morphologically distinct from the more posterior, segmental portions (Fig. 12C; Kitamura

and Shimizu, 2000). A distinct anterior projection with fine branches is seen at a lateral anterior position in the M lineage on each side of the embryo (Figs. 13C, C′); this projection appears to come from a single large cell. By 96 h post-injection, this projection has extended posteriorly along the dorsal aspect and still appears to arise from a single large cell (Figs. 12D, D′); as the segmental mesoderm spreads dorsally, the long projection is contacted by M-derived circumferential fibers (Figs. 12D, D′) followed at 120 h post-injection by other cells of the segmental mesoderm (Figs. 12E, E′). At 144 h post-injection, it is apparent that the 4d lineage labels cells up to and including the mouth (Figs. 12F, F′) as well as an array of thin muscle fibers that extend across the head, converging to a common anchor point on each side (Figs. 12F, F′). Thus, as in *Helobdella*, there is clearly a significant contribution to anterior, non-segmental mesoderm from 4d in *Tubifex*.

Discussion

em cells in Helobdella

We have characterized the fates of the early progeny of the bilaterally paired mesoteloblasts (M teloblasts) which arise from proteloblast DM″ in the leech *Helobdella*. This information is of interest for studies of evolutionary development because cell DM″ is the homolog of micromere 4d, which gives rise to bilateral mesoderm in the embryos of many other spiral cleaving taxa. Thus, comparing features of the 4d lineage among extant spiralians should allow us to draw inferences concerning the condition of the ancestral lophotrochozoan and to elucidate the changes in development associated with the evolution of its diverse descendants.

Our studies reveal that the first six m blast cells (em1–em6), resulting from the stem cell-like divisions of the M teloblasts, contribute to non-segmental tissues of the juvenile leech. em1 and em2 clones contribute the lining of the digestive tract. Clones arising from cells em3, em4 and em5 are similar in that each contributes presumptive radial muscles to the dorsal, lateral and ventral portions of the proboscis, respectively, but there are also clear differences among them: the em3 clone undergoes slow and unequal early divisions that yield a prominent cell with a large nucleus not seen in any other em lineage; em4 and em5 have roughly similar rates of early proliferation, but the em5 clones contribute prominently to the musculature of the proboscis sheath and also contribute a cluster of cells to ganglion R1 which appears to be homologous to the segmental complement of M-derived neurons, neither of which is seen in the em4 clone. Finally, em6 generates a hybrid clone that is similar to those of the sm blast cells in most respects, except that it contributes longitudinal muscle fibers to the outer ring of the proboscis, and does not contribute circumferential muscle to the provisional integument.

Embryonic origins of endoderm

Our finding that cells em1 and em2 contribute to the lining of the intestine raises questions concerning the relationship of this layer to what was previously defined as endoderm (Nardelli-Haefliger and Shankland, 1993; Liu et al., 1998). Our observations (Fig. 8C) suggest that visceral mesoderm arises from sm blast cells (consistent with prior results); thus, we presume that em1 and em2-derived cells underlying the visceral mesoderm are endoderm. In contrast, Nardelli-Haefliger and Shankland showed that intestinal endoderm arises from the syncytial yolk cell derived in part from macromeres A‴, B‴ and C‴, and apparently not from the M lineage, but found little labeling of the endoderm layer when macromeres were injected with a tracer. This discrepancy could be explained by assuming that em1–2 and macromeres A–C all contribute to the endodermal layer and that Nardelli-Haefliger and Shankland injected M teloblasts after the birth of em1 and em2.

Embryonic origins of the proboscis

The proboscis is a complex structure comprising most of the foregut in rhynchobdellid leeches. It has complex embryonic origins as well; previous studies showed that micromeres from all of the first three quartets contribute some cells to the proboscis and to the epithelium of the proboscis sheath, but these contributions failed to account for most cells of the proboscis or for the muscles of its sheath (Fig. 10). Moreover, those previous studies suggested the inner ring of *hedgehog*-expressing cells in the stage 9–10 embryo as precursors of the radial musculature (Kang et al., 2003). Our present work indicates that those inner ring cells, which we propose to be organizers of proboscis development, arise from em1 and em2 and constitute an epithelial lining of the foregut. The radial muscles arise instead from em3–em5.

Contributions of em cells to anterior segments

In contrast to vertebrate and insect embryos, which create segments by establishing boundaries within pre-existing fields of cells, the mesodermal and ectodermal components of segments in leech embryos represent the interdigitation of spatially stereotyped clones, which arise from parallel arrays of lineage-restricted mesodermal and ectodermal founder cells (Weisblat and Shankland, 1985). The fact that most of the seven classes of blast cell clones interdigitate across segment boundaries raises complications at the anterior and posterior ends of the animal; either the terminal segments should be missing cells that would normally be contributed by nonexistent blast cells anterior or posterior to the finite blast cell array, and/or the lineages of the blast cell clones populating the terminal segments must deviate from those contributing to midbody segments. Here, we have shown that the latter possibility applies in the case of the mesodermal lineages contributing to the anterior segments, with the em5 and em6 clones each being hybrid in nature. The em5 clone gives rise to largely non-segmental progeny, but contributes the cluster of mn neurons that would otherwise be missing from segmental ganglion R1. The em6 clone gives rise to a largely normal complement of segmental progeny, including the somite that overlaps the anterior portion of ganglion R1, but also contributes longitudinal muscle fibers to the proboscis.

Comparisons with other spiralians

A goal of the present work is to provide a basis for comparisons with other spiralians aimed at distinguishing conserved and varying features of the 4d lineage associated with body plan evolution in this group. At present, the scope for comparison is limited because detailed lineage information is only available for a few other species.

For glossiphoniid leeches, the M lineages in the congeneric species *H. triserialis* and *H. robusta* contribute prostomial tissues and exhibit “freckle” cells at early stage 8 which arise from the equivalent of cells em1 and em2 in *H. robusta* (Zackson, 1982); (Chi, 1996). No freckle cells were observed in an analysis of early M teloblast progeny in a more distant glossiphoniid species, *Theromyzon rude* (Gleizer and Stent, 1993) rather, the first two m blast cells in *T. rude* were described as contributing to the prostomium and to M-derived neurons in the first two segments, comparable to cells em5 and em6 in our study of *Helobdella*. Whether these cells contributed a lining to the proboscis lumen and gut was not noted. We note that Gleizer and Stent analyzed *T. rude* by direct injection of blast cells visible at the surface of the embryo; thus, it is possible that one or more cells in the early M lineage were not detected in their work.

Leeches and oligochaetes comprise a monophyletic group of annelids, Clitellata (Erseus and Kallersjo, 2004; Zrzavy et al., 2009), and their embryos share many details of early development, including the production of segmental mesoderm and ectoderm from homologous sets of teloblasts (Weisblat and Shankland, 1985; Storey, 1989; Goto et al.,

1999a,b). Early patterns of cell divisions and clone morphologies within the segmental M lineages across clitellate embryos are highly similar; thus, the morphological differences among adults of these species must arise later in development. Will the same hold true for the early, non-segmental contributions of the 4d lineage? Technical considerations prevented us from analyzing the early M lineage in *Tubifex* embryos at the level of detail obtained for *Helobdella*. Nevertheless, it is clear that cell 4d contributes to prostomial mesoderm in both species, and several more specific comparisons can be made between these distantly related clitellate annnelids. In *Tubifex*, there are clearly no freckle cells, but 4d derivatives do line the opening of the mouth. Intriguingly, *Tubifex* embryos examined 72 h after injecting 4d with lineage tracer, exhibit a conspicuous cell with a large flat nucleus at the anterior end of each germinal band that is intriguingly similar in size and position to the cell observed in the em3 clone of *Helobdella*.

Considering more distantly related annelids, an exception to the rule that segmental mesoderm arises from the daughters of 4d has emerged for the polychaete annelid *Capitella teleta* (Meyer et al., 2010). While the *Capitella* 4d lineage gives rise to the primordial germ cells, and several trunk muscles as in other spiralians, the segmental mesoderm arises instead from third quartet micromeres 3d and 3c. In *Helobdella robusta*, the homologous micromeres contribute the circumferential muscles of the proboscis and to a sparsely branching network of cells extending throughout the length of the animal, whose function remains unknown (Huang et al., 2002). For another polychaete, *Platynereis dumerilii*, 4d is described as giving rise to bilateral trunk mesoderm, more typical of the presumed canonical spiralian (Ackermann et al., 2005).

In molluscs as in annelids, cell 4d typically divides bilaterally and contributes progeny to muscle, heart, kidney, intestine and hindgut tissues (Render, 1997; Hejnol et al., 2007). However, in contrast to the uniformly polarized divisions of the M teloblasts seen in clitellate annelids, the homologous mesentoblasts in molluscan embryos (as exemplified by two gastropod species, *Ilyanassa obsoleta* and *Crepidula fornicata*) exhibit reproducible alternations in the polarization of their early divisions: in *Ilyanassa*, the first and third cells are born from the vegetal side of the mesentoblast; the second cell is born from the animal side; and the fourth, fifth and sixth cells arise from the animal side at a more medial position (Swartz et al., 2008; Rabinowitz et al., 2008). Similarly, in *Crepidula*, the first and third cells are born from the vegetal side, while the second and fourth cells arise from the animal side (Henry et al., 2010). As a result, the early mesentoblast progeny are not organized into coherent columns as in the m bandlets of *Helobdella* and *Tubifex* (Swartz et al., 2008; Rabinowitz et al., 2008).

In *Crepidula*, the first and third (vegetally born) cells from each mesentoblast contribute to the intestine, similar to the digestive tract-lining fate of cells em1 and em2 in *Helobdella*. But the second mesentoblast-derived cell in *Crepidula* contributes to an “embryonic kidney” rather than to the gut (Henry et al., 2010). Analogous provisional structures, termed protonephridia, are a general feature of clitellate annelid embryos reviewed in Anderson (1973), including some leeches reviewed in Sawyer (1986); but no such structures have been identified in *Helobdella*, so we could not investigate their origins, and whether or not the annelid protonephridium and the molluscan embryonic kidney are homologous remains to be determined. Assuming that the intestine-forming lineages are homologous in annelids and molluscs, this difference could represent the intercalation of a new cell in the *Crepidula* 4d lineage or the loss of a cell from the *Helobdella* 4d lineage, relative to the ancestor.

Conclusions

In summary, the work presented here for *Helobdella* and *Tubifex* establishes a basis for more detailed comparisons, across diverse spiralian taxa, of the developmental cell fates of micromere 4d, whose status as a precursor of mesodermal tissues is a hallmark of the conserved early development of the super-phylum Lophotrochozoa. We tentatively propose that the very first cell arising from the bilateral daughters of 4d (em1 in our terminology) contributes to the lining of the digestive tract as a general feature of annelids and molluscs, and that further homologies, such as the prominent large cells in the em3 clone can be identified at least within the Clitellata. Elucidating the division patterns and fates in the 4d lineage across spiralians will lead to a better understanding of how evolutionary changes have led to body plan diversification despite the conserved patterns of early development in this large group of animals.

With this present analysis.

Supplementary Material

Refer to Web version on PubMed Central for supplementary material.

Acknowledgments

We would like to thank the Levine and Patel labs for their generosity in sharing their confocal microscopes. We also thank Dr. Dian-Han Kuo for extensive and indispensable discussions, and for editing of the manuscript. This work was supported by NSF grant I0S-0922792 to D.A.W.

References

Ackermann C, Dorresteijn A, Fischer A. Clonal domains in postlarval *Platynereis dumerilii* (Annelida: Polychaeta). J Morphol. 2005; 266:258–280. [PubMed: 16170805]

Anderson, DT. Embryology and Phylogeny in Annelids and Arthropods. Pergamon; Oxford: 1973.

Astrow S, Holton B, Weisblat DA. Centrifugation redistributes factors determining cleavage patterns in leech embryos. Dev Biol. 1987; 120:270–283. [PubMed: 3817294]

Bissen ST, Weisblat DA. The durations and compositions of cell cycles in embryos of the leech, *Helobdella triserialis*. Development. 1989; 106:105–118. [PubMed: 21428107]

Bouche M, Biagianti-Risbourge S, Vernet G. A light and scanning electron microscope study of the morphology of the chaetae of *Tubifex tubifex* in a non-polluted medium. Hydrobiologia. 1997; 411:39–44.

Chi. Freckle cells, a unique population of non-segmental mesoderm found during early leech development. Department of Molecular and Cellular Biology. University of California; Berkeley: 1996. p. 1-20.

Cho SJ, Valles Y, Giani VC Jr, Seaver EC, Weisblat DA. Evolutionary dynamics of the wnt gene family: a lophotrochozoan perspective. Mol Biol Evol. 2010; 27:1645–1658. [PubMed: 20176615]

Desjeux I, Price DJ. The production and elimination of supernumerary blast cells in the leech embryo. Dev Genes Evol. 1999; 209:284–293. [PubMed: 11252181]

Dohle W. The ancestral cleavage pattern of the clitellates and its phylogenetic deviations. Hydrobiologia. 1999; 402:267–283.

Dunn CW, Hejnol A, Matus DQ, Pang K, Browne WE, Smith SA, Seaver E, Rouse GW, Obst M, Edgecombe GD, Sørensen MV, Haddock SH, Schmidt-Rhaesa A, Okusu A, Kristensen RM, Wheeler WC, Martindale MQ, Giribet G. Broad phylogenomic sampling improves resolution of the animal tree of life. Nature. 2008; 452:745–749. [PubMed: 18322464]

Erseus C, Kallersjo M. 18S rDNA phylogeny of Clitellata (Annelida). Zool Scr. 2004; 33:187–196.

Fernández J, Stent GS. Embryonic development of the glossiphoniid leech *Theromyzon rude*: structure and development of the germinal band. Dev Biol. 1980; 78:407–434. [PubMed: 7409309]

Fernández J, Olea N, Téllez V, Matte C. Structure and development of the egg of the glossiphoniid leech Theromyzon rude: reorganization of the fertilized egg during completion of the first meiotic division. Dev Biol. 1990; 137:142–154. [PubMed: 2295361]

Freeman G, Lundelius JW. Evolutionary implications of the mode of D quadrant specification in coelomates with spiral cleavage. J Evol Biol. 1992; 5:205–247.

Gleizer L, Stent GS. Developmental origin of segmental identity in the leech mesoderm. Development. 1993; 117:177–189. [PubMed: 8223246]

Gline SE, Kuo DH, Stolfi A, Weisblat DA. High resolution cell lineage tracing reveals developmental variability in leech. Dev Dyn. 2009; 238:3139–3151. [PubMed: 19924812]

Gonsalves FC, Weisblat DA. MAPK regulation of maternal and zygotic Notch transcript stability in early development. Proc Natl Acad Sci USA. 2007; 104:531–536. [PubMed: 17202257]

Goto A, Kitamura K, Arai A, Shimizu T. Cell fate analysis of teloblasts in the *Tubifex* embryo by intracellular injection of HRP. Dev Growth Differ. 1999a; 41:703–713. [PubMed: 10646800]

Goto A, Kitamura K, Shimizu T. Cell lineage analysis of pattern formation in the *Tubifex* embryo. I Segmentation in the mesoderm. Int J Dev Biol. 1999b; 43:317–327. [PubMed: 10470648]

Hejnol A, Martindale MQ, Henry JQ. High-resolution fate map of the snail *Crepidula fornicata*: the origins of ciliary bands, nervous system, and muscular elements. Dev Biol. 2007; 305:63–76. [PubMed: 17346693]

Hejnol A, Obst M, Stamatakis A, Ott M, Rouse GW, Edgecombe GD, Martinez P, Baguna J, Bailly X, Jondelius U, Wiens M, Muller WE, Seaver E, Wheeler WC, Martindale MQ, Giribet G, Dunn CW. Assessing the root of bilaterian animals with scalable phylogenomic methods. Proc Biol Sci. 2009; 276:4261–4270. [PubMed: 19759036]

Henry JJ, Collin R, Perry KJ. The slipper snail, *Crepidula*: an emerging lophotrochozoan model system. Biol Bull. 2010; 218:211–229. [PubMed: 20570845]

Huang FZ, Kang D, Ramirez-Weber FA, Bissen ST, Weisblat DA. Micromere lineage in the glossiphoniid leech *Helobdella*. Development. 2002; 129:719–732. [PubMed: 11830572]

Jackson JBC, Kirby MX, Berger WH, Bjorndal KA, Botsford LW, Bourque BJ, Bradbury RH, Cooke R, Erlandson J, Estes JA, Hughes TP, Kidwell S, Lange CB, Lenihan HS, Pamdolfi JM, Peterson CH, Steneck RS, Tegner MJ, Warner RR. Historical overfishing and the recent collapse of coastal ecosystems. Science. 2001; 293:629–639. [PubMed: 11474098]

Kang D, Huang F, Li D, Shankland M, Gaffield W, Weisblat DA. A *hedgehog* homolog regulates gut formation in leech (*Helobdella*). Development. 2003; 130:1645–1657. [PubMed: 12620988]

Kitamura K, Shimizu T. Analyses of segment-specific expression of alkaline phosphatase activity in the mesoderm of the oligochaete annelid *Tubifex*: implications for specification of segmental identity. Dev Biol. 2000; 219:214–223. [PubMed: 10694417]

Kramer AP, Weisblat DA. Developmental neural kinship groups in the leech. J Neurosci. 1985; 5:388–407. [PubMed: 3973673]

Kuo DH, Shankland M. A distinct patterning mechanism of the O and P cell fates in the development of the rostral segments of the leech *Helobdella robusta*: implication for the evolutionary dissociation of developmental pathway and morphological outcome. Development. 2004; 131:105–115. [PubMed: 14645128]

Liu NJ, Isaksen DE, Smith CM, Weisblat DA. Movements and stepwise fusion of endodermal precursor cells in leech. Dev Genes Evol. 1998; 208:117–127. [PubMed: 9601984]

Lyons DC, Weisblat DA. D quadrant specification in the leech Helobdella: actomyosin contractility controls the unequal cleavage of the CD blastomere. Dev Biol. 2009; 334:46–58. [PubMed: 19607823]

Meyer NP, Boyle MJ, Martindale MQ, Seaver EC. A comprehensive fate map by intracellular injection of identified blastomeres in the marine polychaete *Capitella teleta*. Evodevo. 2010; 1:8. [PubMed: 20849573]

Nakamoto A, Arai A, Shimizu T. Cell lineage analysis of pattern formation in the *Tubifex* embryo. II Segmentation in the ectoderm. Int J Dev Biol. 2000; 44:797–805. [PubMed: 11128574]

Nardelli-Haefliger D, Shankland M. *Lox10*, a member of the *NK-2* homeobox gene class, is expressed in a segmental pattern in the endoderm and in the cephalic nervous system of the leech *Helobdella*. Development. 1993; 118:877–892. [PubMed: 7915671]

Oda-Ishii I, Bertrand V, Matsuo I, Lemaire P, Saiga H. Making very similar embryos with divergent genomes: conservation of regulatory mechanisms of *Otx* between the ascidians *Halocynthia roretzi* and *Ciona intestinalis*. Development. 2005; 132:1663–1674. [PubMed: 15743880]

Perry SV. Vertebrate tropomyosin: distribution, properties and function. J Muscle Res Cell Motil. 2001; 22:5–49. [PubMed: 11563548]

Pittenger MF, Kazzaz JA, Helfman DM. Functional properties of non-muscle tropomyosin isoforms. Curr Opin Cell Biol. 1994; 6:96–104. [PubMed: 8167032]

Rabinowitz JS, Chan XY, Kingsley EP, Duan Y, Lambert JD. Nanos is required in somatic blast cell lineages in the posterior of a mollusk embryo. Curr Biol. 2008; 18:331–336. [PubMed: 18308570]

Ren X, Weisblat DA. Asymmetrization of first cleavage by transient disassembly of one spindle pole aster in the leech *Helobdella robusta*. Dev Biol. 2006; 292:103–115. [PubMed: 16458880]

Render JA. Cell fate maps in the *Ilyanassa obsoleta* embryo beyond the third division. Dev Biol. 1997; 189:301–310. [PubMed: 9299122]

Sawyer, RT. Leech Biology and Behavior. Clarendon Press; Oxford: 1986. p. 1-1065.

Shimizu, T. Development in the freshwater oligochaete *Tubifex*. In: Harrison, FW.; Cowden, RR., editors. Developmental Biology of Freshwater Invertebrates. Alan R. Liss; New York, NY: 1982. p. 283-316.

Song MH, Huang FZ, Chang GY, Weisblat DA. Expression and function of an *even-skipped* homolog in the leech *Helobdella robusta*. Development. 2002; 129:3681–3692. [PubMed: 12117817]

Storey KG. Cell lineage and pattern formation in the earthworm embryo. Development. 1989; 107:519–531.

Swartz SZ, Chan XY, Lambert JD. Localization of *Vasa* mRNA during early cleavage of the snail *Ilyanassa*. Dev Genes Evol. 2008; 218:107–113. [PubMed: 18214533]

Wedeen CJ, Shankland M. Mesoderm is required for the formation of a segmented endodermal cell layer in the leech *Helobdella*. Dev Biol. 1997; 191:202–214. [PubMed: 9398435]

Weisblat DA, Huang FZ. An overview of glossiphoniid leech development. Can J Zool. 2001; 79:218–232.

Weisblat DA, Shankland M. Cell lineage and segmentation in the leech. Philos Trans R Soc Lond B. 1985; 312:39–56. [PubMed: 2869529]

Zackson SL. Cell clones and segmentation in leech development. Cell. 1982; 31:761–770. [PubMed: 6186389]

Zhang SO, Weisblat DA. Applications of mRNA injections for analyzing cell lineage and asymmetric cell divisions during segmentation in the leech *Helobdella robusta*. Development. 2005; 132:2103–2113. [PubMed: 15788451]

Zrzavy J, Riha P, Pialek L, Janouskovec J. Phylogeny of Annelida (Lophotrochozoa): total-evidence analysis of morphology and six genes. BMC Evol Biol. 2009; 9:189. [PubMed: 19660115]

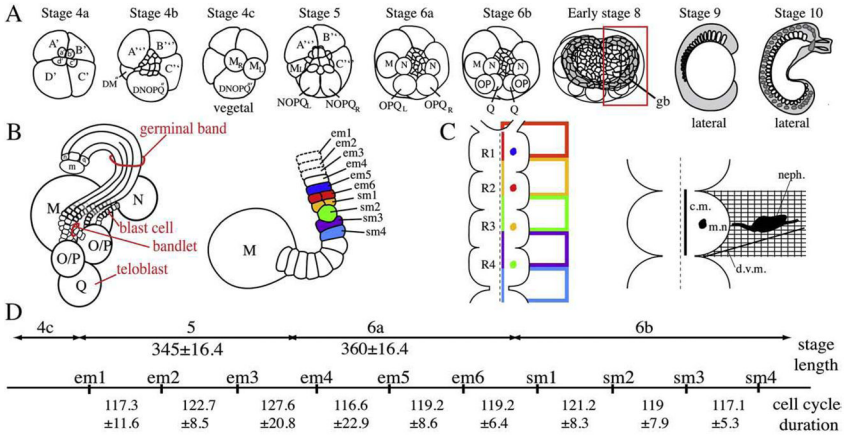

Fig. 1.

Mesoderm development in the leech *Helobdella*. A. Representations of selected developmental stages (animal pole views unless otherwise indicated; see text for details). B. Left: schematic showing the relationships of teloblasts, blast cells, bandlets, and germinal band on the right side of an early stage 8 embryo, corresponding to the boxed section in panel (A). Right: schematic showing an M teloblast and its descendant column of em and sm cells, roughly 34 h after the division of DM″; em1–3 are depicted with dashed outlines because the timing and orientation of their first mitoses are unknown; em4 (black outline) has not yet divided at this time, nor has em5 (blue), but em6 (red) and sm1 (yellow) have each undergone bilateral divisions; sm2 (green) is shown rounding up for mitosis while sm3 (turquoise) and sm4 (purple) have not yet divided. C. Left: distribution of em and sm clones across segments R1–R4 (color coded as in B; cells em1–em4 do not contribute to segmental mesoderm). Shown are ganglia R1–R4 (black contours): dashed line marks the midline; colored lines next to the midline indicate muscle cells within the nerve cord; colored circles indicate clusters of M-derived neurons; open boxes, partially obscured by the ganglia, depict hemi-somite boundaries. Right: schematic modified from (Weisblat and Huang, 2001) depicting the mesodermal progeny (elements of 3 sm clones) associated with a typical midbody segment; c.m., connective muscle, m.n., M-derived neurons, d.v.m. dorsoventral muscle, neph. nephridium, hatched lines represent body wall muscles. D. Six cells are born from each M teloblast prior to stage 6b. Durations (in minutes) of relevant developmental stages and M teloblast cell cycles, compiled from time-lapse movies of embryos (Supplemental Movie 1). Cell cycles and stage lengths were calculated and averaged from a total of 13 experiments. Anterior is up in this and all subsequent figures unless otherwise noted. (For interpretation of the references to color in this figure legend, the reader is referred to the web version of this article.)

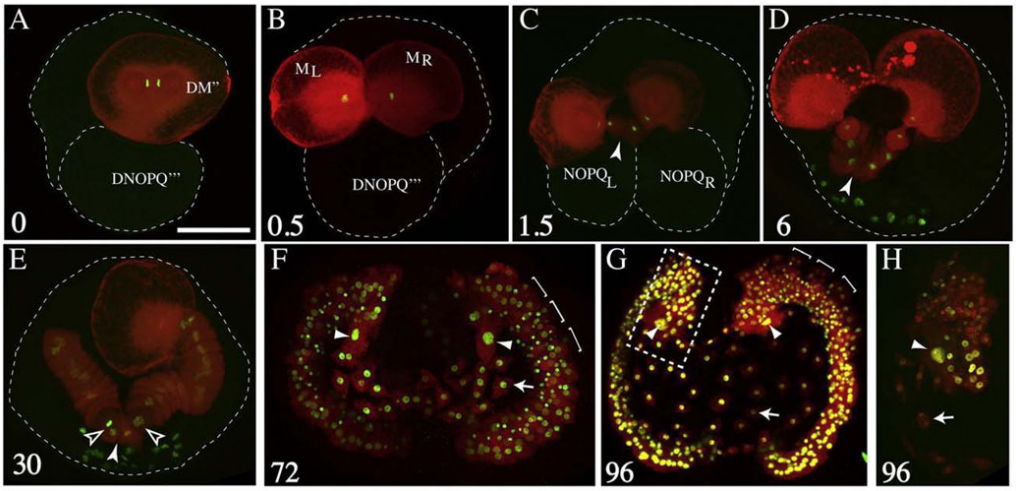

Fig. 2.

M lineage during cleavage and segmentation. (A–E). Confocal images (maximally projected stacks) of embryos in which DM″ was injected with RDA (red) at stage 4b; injected embryos were fixed after the time intervals indicated (hours post-injection), then counterstained by immunofluorescence for histone H1 to label nuclei (green). For orientation, cell and/or embryos contours are indicated by dotted lines. A. Bilateral division of DM″ gives rise to teloblasts M_L and M_R. B. During interphase, nuclei of M_L and M_R remain close to the zone of contact between the two cells. C. As shown previously (Fernández and Stent, 1980), the first progeny of M_L and M_R (em1 cells) arise in direct apposition at the site of contact, so the distal (prospective anterior) ends of the m bandlets are connected at this time (arrowhead in C–E). D. The anterior contact between left and right m bandlets (arrowhead) is maintained as subsequent em cells are born. E. By 30 h post-injection, the columns of primary blast cells fromeach teloblast have lengthened and anterior cells havebegun to divide (open arrowheads; M_L is not present in this stack of images). (F–H). Confocal images of older embryos in which DM″ was injected with RDA plus pEF-H2B:GFP or *h2bgfp* mRNA to specifically label M lineage nuclei (green). F. By 72 h post-injection, proliferation within sm blast cell clones has given rise to repeated clusters of cells (hemisomites; brackets). Anterior/distal to the hemisomites, the distribution of labeled cells is markedly different, including a population of dispersed “freckle cells” (e.g., arrow) between the left and right germinal bands and a large cell with a prominent nucleus at the anterior end of each germinal band (arrowheads). G. By 96 h post-injection, segmentation in the anterior M lineage is more obvious (brackets), freckle cells are scattered across the prospective dorsal side of the embryo (e.g., arrow) and there is still a large prominent cell at the anterior of each germinal band (arrowheads). H. Enlarged view of a sibling embryo, corresponding to the boxed area of (G) showing the large anterior cell (arrowhead) and freckle cells, one of which was dividing (arrow). Scale bar, 130 mm in A–E; 100 mm in F–G; 60 mm in H. (For interpretation of the references to color in this figure legend, the reader is referred to the web version of this article.)

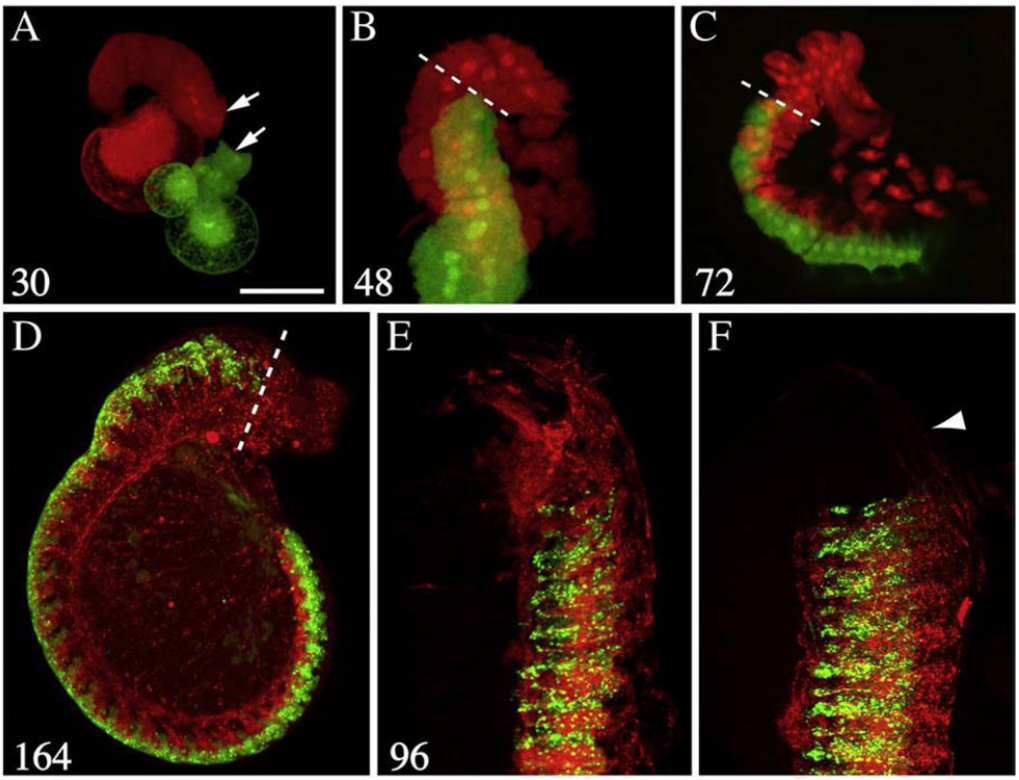

Fig. 3.

Mesodermal and ectodermal lineages begin segmental blast cell production at approximately the same time. (A–E) Confocal images (maximally projected stacks) of embryos injected with RDA (red) into newborn M_L teloblasts (stage 4c) and with FDA (green) into newborn OP_L proteloblasts (stage 6b); embryos were fixed at the time intervals indicated (hours after the M injection). A. At 30 h post-injection, the columns of cells (arrows) arising from the M and OP lineages are not yet in contact. B. By 48 h post-injection the two columns of cells are roughly parallel, but the M teloblast derivatives extend well beyond the anterior extent of the OP lineage (dashed line in B–D). C. The mismatch between the anterior borders of the M and OP lineages persists as the freckle cells spread between the germinal bands. D. By stage 9, a lateral view (ventral to left) reveals many RDA-labeled cells in the prostomium anterior to the OP lineage. E. Confocal image of the germinal plate dissected from an embryo fixed 96 h post-injection shows extensive mesodermal progeny anterior to the OP lineage. F. A dissected germinal plate comparable to that shown in (E), but from an embryo in which the M teloblast and OP proteloblast were injected within minutes of one another, at the birth of OP (stage 6b). With this injection paradigm, the anterior M and OP boundaries fall within the same segment as shown here, or in adjacent segments (not shown). In this preparation, some RDA-labeled contractile fibers from the provisional integument (arrowhead) appear above the segmental derivatives, due to folding of the preparation during mounting. Scale bar, 60 mm in A–C; 80 mm in D–F. (For interpretation of the references to color in this figure legend, the reader is referred to the web version of this article.)

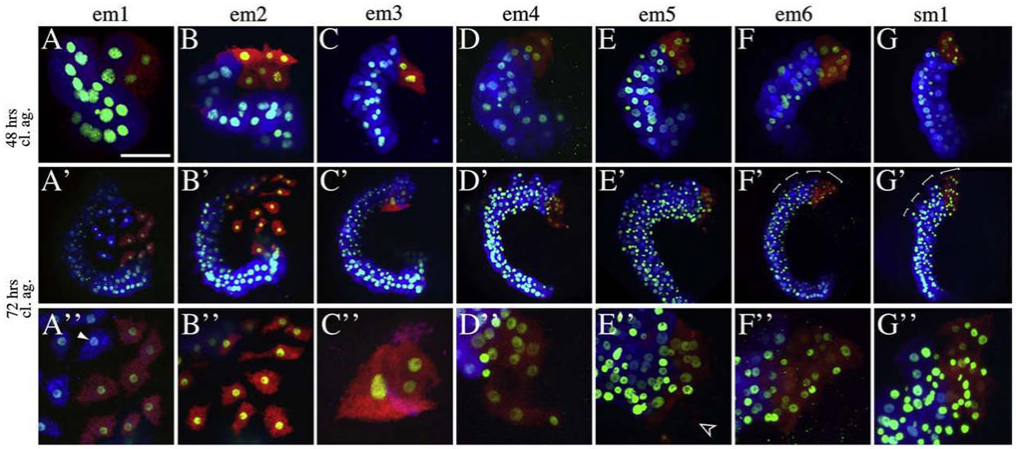

Fig. 4.

Lineage-specific distribution patterns of early em clones. Confocal images (maximum projections of stacks) of embryos in which timed tandem injections (see text for details) were performed to uniquely label the progeny of cells em1-6 or sm1 with RDA (red) and either *h2bgfp* mRNA or pEF-H2B:GFP (yellow green). Cells arising after the second injection also contain ADA (blue). Embryos were cultured for 48 (top row) or 72 (middle and bottom rows) h post-injection, then fixed and processed for microscopy. Bottom panel in each column shows close-up views of the uniquely labeled clones in the middle panel. The founder cell for each uniquely labeled clone is indicated above the column. In A′ and A ″, note the similarity between the blue, em2-derived (arrowhead in A″) and red, em1-derived freckle cells. In E″, note cell debris (open arrowhead) suggestive of cell death in the em5 clone. In F′ and G′, note lateral expansion of hemisomites (brackets). See text for details. Scale bar, 60 mm in A–G; 100 mm in A′–G′; 25 mm in A″–G″.

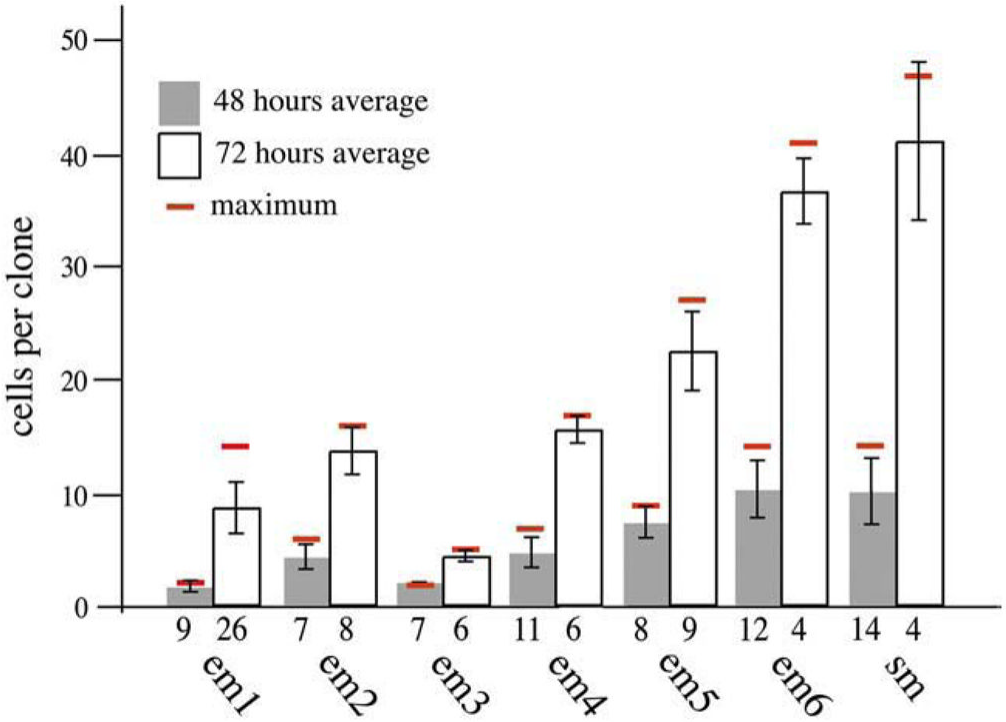

Fig. 5.

Lineage-specific differences in proliferation within em clones. Cells in uniquely labeled clones from timed tandem injections as shown in Fig. 4 were counted. Standard deviations are indicated by error bars. Maximum clone sizes are indicated in red. Sample sizes are indicated below the bars. (For interpretation of the references to color in this figure legend, the reader is referred to the web version of this article.)

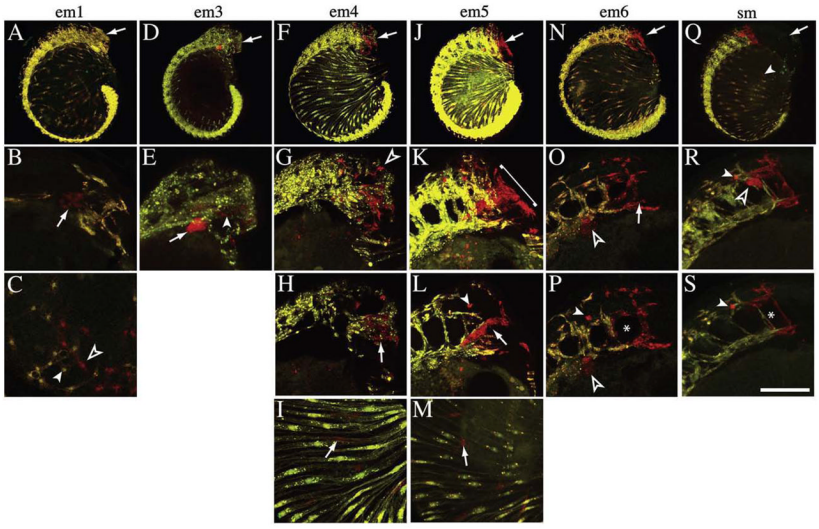

Fig. 6.

Lineage-specific distribution patterns of em clones at early stage 9. Confocal images (maximum projections of stacks, lateral views, ventral to left) of embryos in which timed tandem injections were used to uniquely label em (or sm) clones as in Fig. 4, except that in these experiments, FDA (yellow green) was used for the second injection, no nuclear label was used, and injected embryos were cultured to early stage 9, by which time the morphological differentiation of anterior tissues was underway. The top image in each column shows the complete stack of optical sections (arrows indicate the proboscis tip); images below include sections highlighting the uniquely labeled clone. A–C. em1 contributes progeny to the nascent proboscis in the medial portion of the prostomium (arrow in B); more posteriorly, em1 progeny (open arrowhead in C) lie superficial to the syncytial yolk cell, in a plane beneath the circumferential muscle fibers of the provisional integument (visible in A but not C); em2 makes similar contributions (closed arrowhead in C) and the uniquely labeled em2 clone is not included in this figure. D, E. em3 contributes a brightly labeled patch (arrow in E, suggesting that there have been few divisions in this sub-lineage), and presumptive muscle fibers within the proboscis (closed arrowhead in E). F–I. em4 contributes scattered cells in the prostomium (open arrowhead in G), musculature in the developing proboscis (arrow in H), and cells scattered among the circumferential muscle fibers of the provisional integument (arrow in I). J–M. em5 contributes muscle fibers to the presumptive proboscis sheath (bracket in K), muscle fibers to the presumptive proboscis (arrow in L), a cluster of neurons in ganglion R1 (closed arrowhead in L) and superficial cells among the circumferential muscle fibers of the provisional integument (arrow in M). N–P. em6 contributes longitudinal muscle fibers to the proboscis (arrow in O), a lateral patch of cells in segment R3 (open arrowhead in O and P), mesoderm surrounding the first coelomic cavity (asterisk in P) and a cluster of neurons in ganglion R2 (closed arrowhead in P). Q–S. An anterior sm clone contributes circumferential muscle fibers to the provisional integument (closed arrowhead in Q), a nephridial primoridum (open arrowhead in R), a cluster of neurons in the next posterior ganglion (closed arrowhead in R and S) and the mesoderm surrounding the coelom (asterisk in S). Scale bar, 180 mm in A, D, F, J, N, and Q; 50 mm in all other panels.

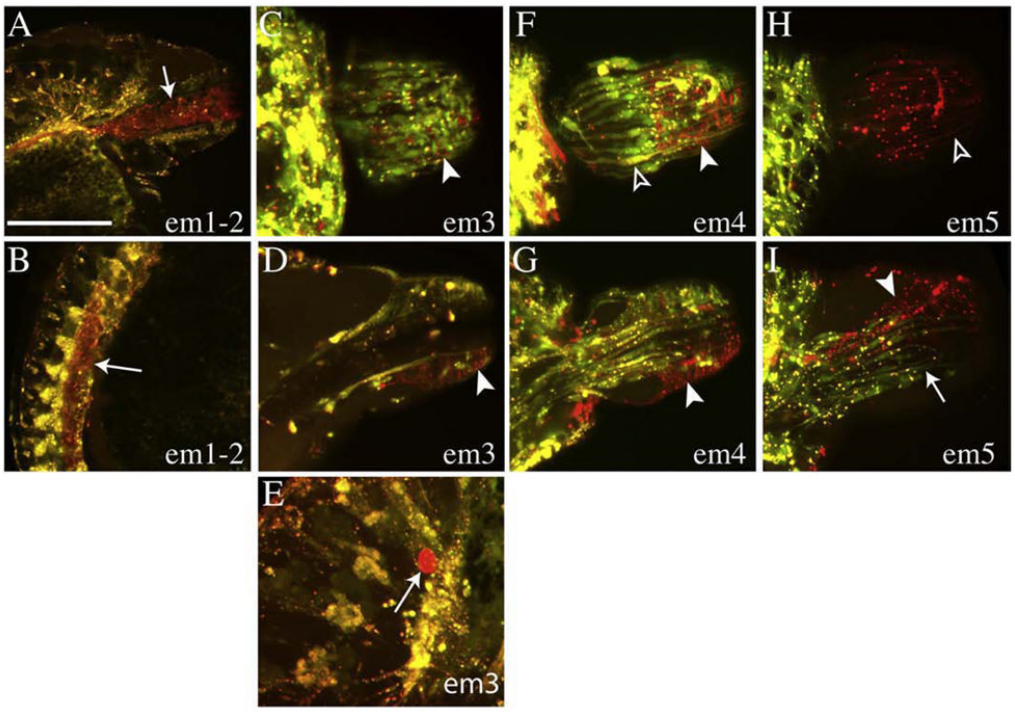

Fig. 7.

Definitive contributions of em lineages. Confocal images (maximal projections of stacks, lateral views) of embryos with uniquely labeled em clones as in Fig. 6, except that: 1) in some embryos the injections were timed so both em1 and em2 were labeled with RDA only and; 2) the injected embryos were cultured to late stage 9, by which time differentiation in anterior tissues is well advanced, although the proboscis is still in its everted configuration. A–B. em1 and em2 progeny line the lumen of the proboscis (arrow in A) and contribute to a layer of cells between the syncytial yolk cell and the germinal plate (arrow in B). C–D. lateral and medial optical sections, respectively, show that em3 contributes radial muscle fibers to lateral (arrowhead in C) and dorsal (arrowhead in D) sectors of the proboscis. E. em3 also gives rise to a brightly labeled clump of seemingly detached cells observed at various positions within the germinal plate lateral to segmental mesoderm (arrow). F–G. Lateral and medial optical sections, respectively show that em4 contributes radial muscle fibers to lateral (arrowhead in F) and dorsolateral (arrowhead in G) sectors of the proboscis, just beneath the musculature of the sheath (open arrowhead F). H–I. Lateral and medial optical sections, respectively, show that em5 gives rise to the majority of the musculature in the proboscis sheath (open arrowhead in H) and to radial muscle fibers in the ventral sector of the proboscis (arrowhead in I). Double-labeled longitudinal proboscis muscle fibers (arrow in I) are derived from em6 (not illustrated as a uniquely labeled clone). Scale bar, 25 mm in E; 50 mm in all other panels.

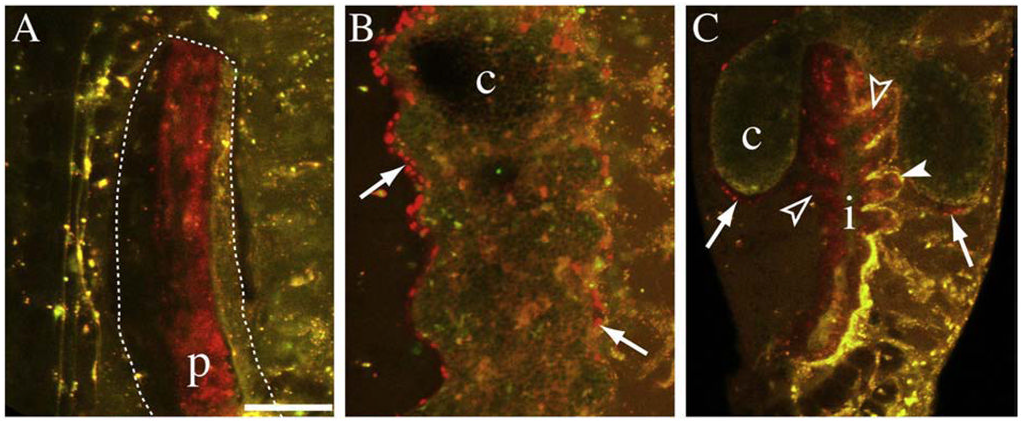

Fig. 8.

em1 and em2 derivatives line the foregut and midgut. Confocal images (maximum projections of stacks) from embryos in which the combined em1 and em2 clones from one M lineage were both labeled with RDA (red) by timed tandem injections. The injected embryos were cultured to stage 11, by which time the digestive tract was well-differentiated. A. By stage 11, the proboscis (p; foregut; dotted contour) has assumed its position within the anterior body; em1 and em2 progeny line both sides of the lumen. B, C. The crop (c; anterior midgut) and intestine (i; posterior midgut) have differentiated from the syncytial yolk cell; em1 and em2 contribute bilaterally to a population of cells lining both the crop (arrows B and C), and the intestine (open arrowheads C). Note that M progeny born after em1 and em2 (double labeled cells, yellow, presumably from sm clones) contribute visceral mesoderm (closed arrowhead) lying just outside the em1 and em2 progeny. Scale bar, 20 mm in A, B; 30 mm in C. (For interpretation of the references to color in this figure legend, the reader is referred to the web version of this article.)

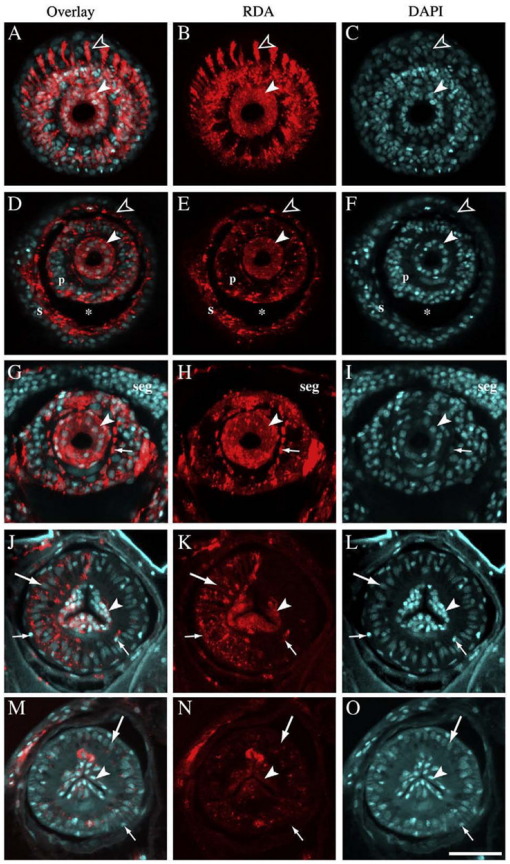

Fig. 9.

The M lineage contributes to all layers of the proboscis and its sheath. Confocal images (maximum projections of stacks from thick sections) showing transverse views (dorsal up) of the proboscises of embryos in which cell DM″ (A–I, M–O) or M_L (J–L) was injected with RDA (red); injected embryos were fixed at stage 9 (Oda-Ishii et al., 2005) or 10 (J–O), counterstained with DAPI (cyan), embedded and sectioned by hand. A–C. At the distal tip of the proboscis, muscle fibers from the sheath (open arrowheads in A–F) connect to the proboscis itself. At this stage, the inner ring comprising em1 and em2 derivatives (closed arrowheads in all panels), is a cylinder of columnar epithelium. D–F. A slightly more posterior section from the same specimen reveals the space (asterisk) between the proboscis (p) and its sheath (s). G–I. Further posterior, at the level of the supraesophageal ganglia (seg), presumptive longitudinal muscle fibers appear as a ring of puncta (small arrows in G–O) surrounding the inner ring. J–L. By mid-stage 10, the proboscis has retracted to within the body cavity and the tri-radiate organization of the lumen is evident. Radial muscles (large arrows in J–O) span from just within the longitudinal muscles at the outer edge of the proboscis to the inner ring and their large ovoid nuclei are shifting toward the outer edge. If the longitudinally oriented cells surrounding the inner ring at stage 9 (small arrows in G–I) are precursors of the peripheral longitudinal muscle fibers at stage 10 and beyond, they must migrate peripherally; candidates for such migrating cells are visible in this section (small arrows). M–O. By late stage 10, nuclei of the longitudinal and radial muscles are arranged in concentric rings near the outer surface of the proboscis. Cells of the inner ring constitute a thin layer lining the tri-radiate lumen. Scale bar, 25 mm. (For interpretation of the references to color in this figure legend, the reader is referred to the web version of this article.)

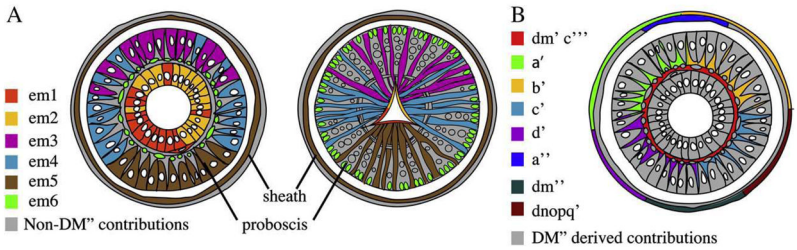

Fig. 10.

Embryonic origins of cells in the proboscis. Drawings depict transverse sections with dorsal up. A. Schematic showing contributions of em clones to the late stage 9 proboscis (left) and a hypothesis of how they relate to cells in the adult proboscis (right), based on the work presented here. In the adult proboscis (right), progeny of em1 and em 2 line the lumen, those of em3–5 comprise radial muscle fibers and those of em6 comprise longitudinal muscle fibers. In these lefthand drawings, grey outlines depict cells not arising from the M lineage, including presumptive nerves and salivary ductules running between the radial muscle fibers and a band of circumferential muscle fibers lying partway out along the radius. B. A schematic based on previously published work in another *Helobdella* species (Huang et al., 2002; Kang et al., 2003) shows contributions from other embryonic lineages accounting for the non-M-derived cells in the stage 9 proboscis.

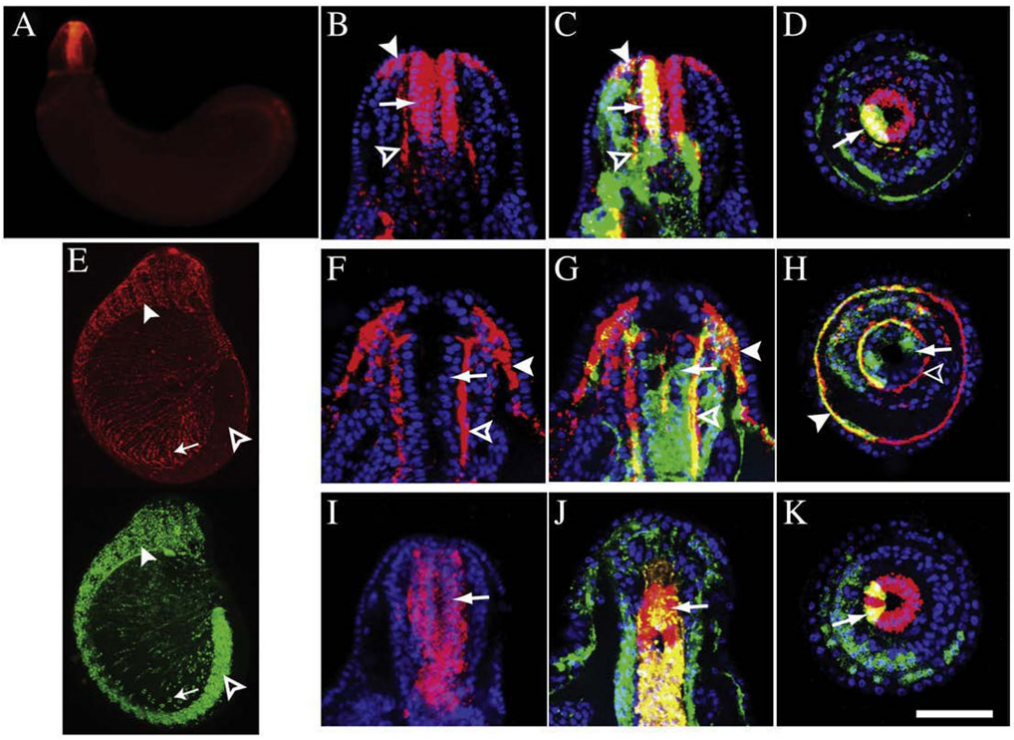

Fig. 11.

Differential expression of hedgehog (*Hau-hh*) and tropomyosins (*Hau-trop1*, *Hau-trop2*) in the developing proboscis. Standard fluorescence (A) and confocal images (maximum projections of stacks; B–K) of embryos in which early M_L teloblasts (stage 4c) were injected with FDA (green); injected embryos were fixed at stage 9–10, processed for fluorescent in situ hybridization (FISH, red), then examined in wholemount or as sections counterstained with DAPI (blue). A–D. FISH for *Hau-hh*. A. Lateral view; expression is predominantly in core of the proboscis (Kang et al., 2003). B. Saggital section through the proboscis shows that *Hau-hh* expression is strongest in cells of the inner ring (arrows), cells just outside the inner ring (open arrowheads) and cells in the epidermal layer at the tip of the proboscis sheath (closed arrowheads). C, D. Saggital and transverse views, respectively showing colocalization of lineage tracer and FISH product (yellow) confirm that *Hau-hh* positive cells are those of the inner ring, derived from em1 and em 2. E–H. FISH for *Hau-tropo1*. E. In stage 9 embryos, *Hau-tropo1* is expressed in the M-derived provisional circumferential muscle fibers of the integument (arrows) and in segmental muscle cells of anterior, more differentiated segments (closed arrowheads), but not in the posterior segmental mesoderm (open arrowheads) where segmental muscles have not yet differentiated. F–H. Saggital and transverse sections (as in B–D) show that *Hau-trop1* is expressed in muscles of the proboscis sheath (closed arrowheads), and in cells just outside the inner ring (open arrowheads), but not in the inner ring (arrows). I–K. In contrast to *Hau-trop1*, *Hau-trop2* is expressed throughout the inner ring of em1 and em 2-derived cells (arrows). Scale bar, 125 mm in A, E; 40 mm in all other panels. (For interpretation of the references to color in this figure legend, the reader is referred to the web version of this article.)

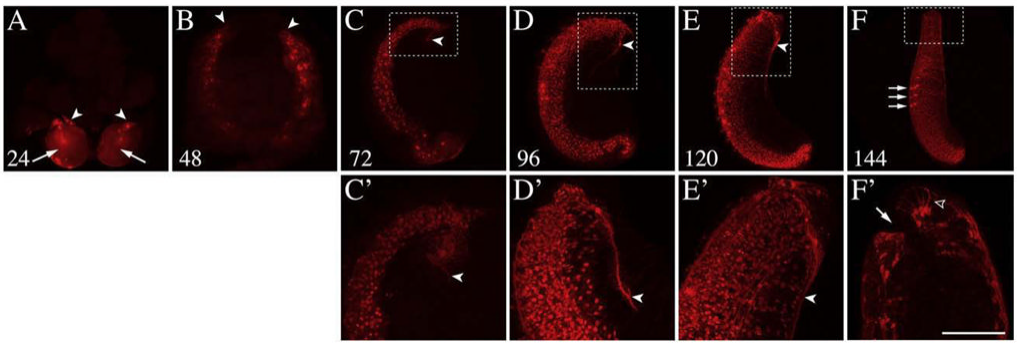

Fig. 12.

Ontogeny of 4d lineage in *Tubifex*. Confocal images (maximum projections of stacks) of *Tubifex* embryos fixed 24–144 h after cell 4d was injected with RDA (red). A, B. Animal views. All others are lateral views (ventral to left). A. 24 h post-injection, M_L and M_R are visible (arrows); the nascent columns of blast cells are not in contact at their distal ends (arrowheads). B. 48 h post-injection, left and right germinal bands are visible, still without contact at their distal ends (arrowheads). C–E, C′–E′. During the period 72–120 h post-injection, a single large 4d-derived cell is evident on each side (arrowheads C′–E′), reminiscent of the large, em3-derived cells in *Helobdella*. C′–E′. Higher power views of the boxed regions in C–E, respectively, show that this large cell appears to form a long process with profuse, fine lateral branches extending posteriorly in dorsolateral territory (closed arrowheads in C′–E′). This cell appears to mark the edge of the dorsally expanding germinal plate. F. By 144 h post-injection, primordial germ cells are visible as three bright clusters of RDA-containing cells (arrows). F′. Magnified view of the anterior end shows that, as in *Helobdella*, the 4d lineage has contributed muscle cells (open arrowhead) anterior to the mouth, and cells lining the mouth opening (arrow). Scale bar, 150 mm in A, B; 200 mm in C–E; 320 mm in F; 60 mm in C′–F′. (For interpretation of the references to color in this figure legend, the reader is referred to the web version of this article.)